

Frontiers in Rotational Spectroscopy: Shapes and Tunneling Dynamics of the Four Conformers of the Acrylic Acid–Difluoroacetic Acid Adduct**

Gang Feng, Qian Gou, Luca Evangelisti, and Walther Caminati*

Abstract: The rotational spectra of four conformers of the acrylic acid–difluoroacetic acid adduct ($\text{CH}_2=\text{CHCOOH}-\text{CHF}_2\text{COOH}$, AA-DFA) are reported and information on their internal dynamics is supplied. This represents an unprecedented result for the conformational analysis, with microwave spectroscopy, of such a heavy molecular adduct.

A carboxylic acid dimer (formic acid–trifluoroacetic acid) was the first adduct observed by microwave (MW) spectroscopy (low resolution), and important structural effects were already determined more than fifty years ago.^[1] However, no information on proton transfer tunneling or on the detection of conformers has been reported on this kind of molecular systems up to a couple of years ago.

Only one conformer could exist, indeed, for the first three carboxylic acid dimers investigated by Fourier transform (FT) MW spectroscopy (trifluoroacetic acid combined with formic acid, or acetic acid, or cyclopropane carboxylic acid),^[2] while the coupling of the CF_3 heavy top internal rotation with the proton transfer did not allow the observation of tunneling splittings.

Tunneling splittings because of proton transfer have been first observed with other techniques than MW spectroscopy, such as femtosecond degenerate four-wave mixing and Raman spectroscopy. The proton transfer rate has been investigated mainly for the prototype system, the formic acid dimer.^[3] Interesting results have been obtained on the ground and first electronic excited states of the benzoic acid dimer^[4] by rotationally resolved laser-induced fluorescence.

Splittings because of the proton tunneling have been reported by FTMW spectroscopy only very recently: in 2010 for formic acid–propionic acid,^[5] in 2011 for formic acid–acetic acid,^[6] in 2012 for the homodimer of acrylic acid^[7] and for the heterodimer benzoic acid–formic acid.^[8] For the two latter molecules the tunneling splittings have been useful to calculate the barrier to proton transfer by using a three-dimensional flexible model.

Reports on the conformational equilibria in dimers of carboxylic acids have been available only during the current year, regarding two conformers of acrylic acid–formic acid^[9] and acrylic acid–trifluoroacetic acid,^[10] and three conformers of acrylic acid–fluoroacetic acid.^[11] Plenty of data concerning many isotopologues of these adducts allowed to quantify the $\text{OH}\rightarrow\text{OD}$ isotopic substitution effect (Ubbelohde effect) on molecular structure.^[12]

AA-DFA is a carboxylic acid dimer which can exist in several conformations. Both monomers, AA and DFA, exist indeed in two stable forms with similar energies,^[13,14] as shown in the upper part of Figure 1, where ΔE is the energy

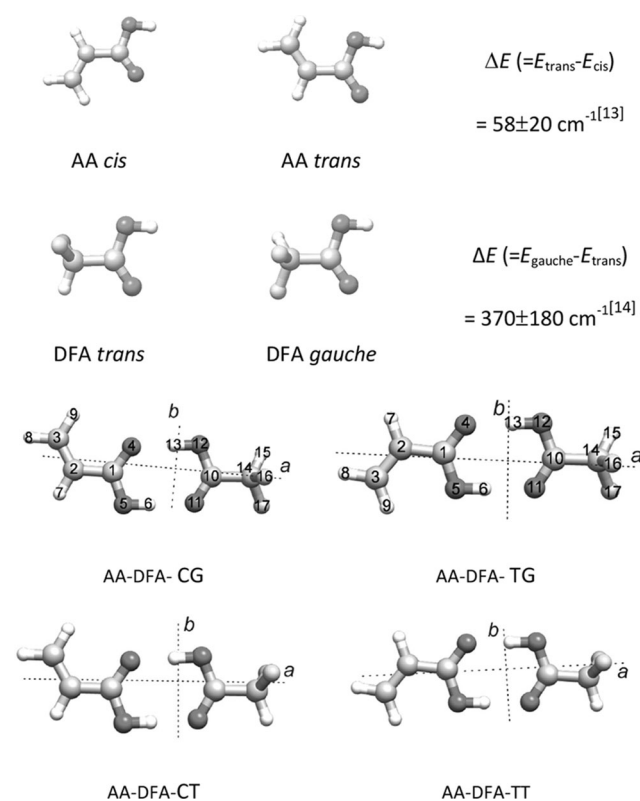


Figure 1. Molecular sketch of the AA and DFA monomers and of their hetero dimers. CT (*cis-trans*), CG (*cis-gauche*), TG (*trans-gauche*), and TT (*trans-trans*) are the four most stable conformations of AA-DFA.

difference between the two conformers in their vibrational and rotational ground states. Thus their 1:1 complex is expected to display four different conformers: *cis-trans* (CT), *cis-gauche* (CG), *trans-gauche* (TG), and *trans-trans* (TT), as drawn at the bottom of Figure 1.

[*] Dr. G. Feng, Q. Gou, Dr. L. Evangelisti, Prof. Dr. W. Caminati
Department of Chemistry, University of Bologna
Via Selmi 2, 40126 Bologna (Italy)
E-mail: walther.caminati@unibo.it

[**] We thank Italian MIUR (PRIN project 2010ERFKXL_001) and the University of Bologna (RFO) for financial support. G. Feng and Q. Gou also thank the China Scholarships Council (CSC) for scholarships.

Supporting information for this article is available on the WWW under <http://dx.doi.org/10.1002/anie.201308459>.

Table 1: MP2/6-311++G(d,p) calculated spectroscopic parameters of the plausible conformers of AA-DFA.

Parameters	CT	CG	TT	TG
A [MHz]	3114.5	3257.5	3489.4	3216.0
B [MHz]	381.0	381.8	370.7	380.9
C [MHz]	361.8	358.4	356.9	358.2
μ_a [D]	2.8	2.9	−3.0	−2.8
μ_b [D]	−0.9	1.3	1.5	−0.8
μ_c [D]	0.0	−1.1	0.0	−0.9
ΔE , $\Delta E_{CP}^{[a]}$ [cm ^{−1}]	0, 0	14, 44	101, 83	101, 108
E_D , $E_{D,CP}^{[b]}$ [kJ mol ^{−1}]	66, 52	66, 52	68, 53	67, 53

[a] Absolute energy values without and with counterpoise correction are −693.283376 and −693.278041 E_h , respectively. [b] E_D and $E_{D,CP}$ are the dissociation energies without and with counterpoise corrections, respectively.

We performed MP2/6-311++G(d,p) geometry optimization calculations of these four forms by using the Gaussian03 program package.^[15] They confirmed the shapes of the four conformers and produced the spectroscopic parameters collected in Table 1. The inclusion of the counterpoise corrections slightly modified the values of the dissociation energies.^[16]

Below we present the obtained results. The experimental details are given in the Supporting Information.

All conformers appear to have similar sets of rotational constants (the maximum difference, about 10 %, is between the A values of CT and TT) and high values of the μ_a dipole moment components. For this reason we started our spectral search in the frequency range where the J 11←10 μ_a -R-type band was expected to fall. The corresponding survey scan is shown in Figure 2, where also lines due to the dimers of the two carboxylic acids, and to their complexes with water appear. We could rapidly assign the component lines of this band of all four conformers. Then several other μ_a and μ_b -type transitions were measured. Interestingly, for the CG and TG forms, each transition was split into two lines because of the internal rotation of the $-\text{CHF}_2$ group. For these two con-

formers, also μ_c -type lines were observed and measured, and the size of their splittings was almost constant (about 2.6 and 6.4 MHz for CG and TG, respectively).

The measured frequencies were fitted by using Pickett's SPFIT program,^[17] according to the Hamiltonian given in Equations (1) for CT and TT forms and (2) for CG and TG forms, respectively.

$$H = H^R + H^{\text{CD}} \quad (1)$$

$$H = \sum_i H_i^R + H^{\text{CD}} + \Delta E_{0^+0^-} + F_{bc} (P_b P_c + P_c P_b) \quad (2)$$

H^R and H^{CD} represent the rigid rotational part and the centrifugal distortion contributions, respectively. In Equation (2), i values run over the symmetric (0^+) and anti-symmetric (0^-) tunneling states, $\Delta E_{0^+0^-}$ is the energy difference between the 0^+ and 0^- states and F_{bc} is a Coriolis coupling constant.

The S reduction and F representation have been used for all fits.^[18] The determined spectroscopic parameters were collected in Table 2 for the CT and TT forms and in Table 3 for the CG and TG forms, respectively. According to Equation (2), two sets of rotational constants are given for the CG and TG species, one for the 0^+ and one for the 0^- sublevels. A common set of centrifugal distortion constants has been determined for the two states. The F_{bc} parameter could not be determined for the CG conformer, as often it

Table 2: Experimental spectroscopic parameters of the C_s forms of AA-DFA, CT, and TT.

	CT	TT
A [MHz]	3143.2651(6) ^[a]	3486.405(2)
B [MHz]	385.3932(2)	376.2862(3)
C [MHz]	366.2331(2)	362.1141(2)
D_J [kHz]	0.0192(7)	0.0179(9)
D_{JK} [kHz]	0.183(6)	0.447(9)
d_2 [Hz]	3.3(2)	3.4(4)
$\sigma^{[b]}$ [kHz]	2.7	2.1
$N^{[c]}$	51	32

[a] Error in parentheses in units of the last digit. [b] Root-mean-square (RMS) error of the fit. [c] Number of lines in the fit.

Table 3: Experimental spectroscopic parameters of the C_1 forms of AA-DFA, CG, and TG.

	CG		TG	
	0^+	0^-	0^+	0^-
A [MHz]	3280.17(5) ^[a]	3279.64(5)	3263.60(4)	3261.90(4)
B [MHz]	388.0466(3)	388.0466(3)	386.975(3)	386.975(3)
C [MHz]	359.3030(3)	359.3028(3)	359.152(3)	359.153(3)
D_J [kHz]	0.0157(9)		0.0174(8)	
D_{JK} [kHz]	0.038(6)		−0.034(8)	
D_K [MHz]	−0.12(5)		−0.21(4)	
$\Delta E_{0^+0^-}$ [MHz]	1.316(6)		3.43(2)	
F_{bc} [MHz]	–		1.05(4)	
$\sigma^{[b]}$ [kHz]	2.6		4.2	
$N^{[c]}$	76		66	

[a] Error in parentheses in units of the last digit. [b] RMS error of the fit. [c] Number of lines in the fit.

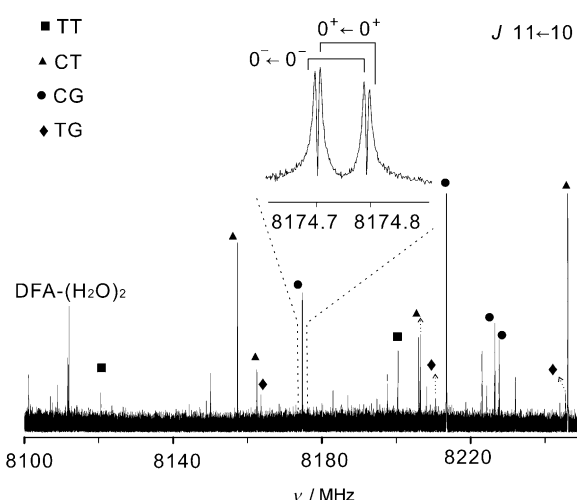


Figure 2. Survey scan of the J 11←10 μ_a -R-type band. The $11_{0,11}$ – $10_{0,10}$ transitions of CG is shown in the inset. The tunneling splitting is 12 kHz, while the Doppler separation is about 100 kHz.

happens in case of small tunneling splittings. The ΔE_{0+0} -quantities are about half of the above-mentioned splitting observed in the μ_c interstate transitions.

The experimental rotational constants resulted quite close to the theoretical values, with a maximum discrepancy of about 1 % for the *A* rotational constant of the TG species. We will see that this discrepancy is mainly imputable to a correction needed for the dihedral angle H15C14-C10O12 describing the rotation of the -CHF₂ lateral group.

Then we investigated the three deuterated species for each conformer, which are AA-DFA(OD), AA(OD)-DFA, and AA(OD)-DFA(OD), except that AA(OD)-DFA(OD) species of TT form because it was too weak to be measured. No tunneling splittings have been resolved. The fits were performed as for the parent species of CT and TT according to the Hamiltonian given in Equation (1). The obtained results, as well as the measured transitions for all the species, are given in the Supporting Information. We could not use the determined rotational constants to obtain structural information on the location of the hydrogen atoms involved in the hydrogen bonds, because of the Ubbelohde effect, that is the increase of the distance between the two monomers upon H→D substitution. The changes of the moments of inertia associated to such effect overwhelm the variations due to the isotopic substitution.

However, in turn, we could use these data to size the Ubbelohde effect. Let us consider the values of the P_{aa} planar moments of inertia, defined as $P_{aa} = \sum_i m_i a_i^2$ and easily obtained from the rotational constants through Equation (3).

$$P_{aa} = h / [(16\pi^2)(-1/A + 1/B + 1/C)] \quad (3)$$

These quantities give a measure of the mass extension along the *a* axis. We report in Table 4 their experimental and calculated shifts (ΔP_{aa}) in going from the parent to the mono- or bideuterated species. The calculated values are obtained from the model structure. The enormous discrepancies

Table 4: Calculated and experimental shifts (ΔP_{aa}) of the P_{aa} planar moments of inertia upon OD deuteration for the CT, TT, CG and TG conformers of AA-DFA.

		CT	ΔP_{aa} [$\mu\text{Å}^2$] TT	CG	TG
AA(OD)-DFA	Exp	2.365	3.142	2.685	2.631
	Calc	0.926	1.216	0.681	1.019
AA-DFA(OD)	Exp	2.929	2.914	2.037	2.876
	Calc	0.019	0.000	0.067	0.013
AA(OD)-DFA(OD)	Exp	5.081		4.587	5.30
	Calc	0.943		0.764	1.031

between the experimental and calculated values are due to the above-mentioned increase of the distance between the two monomers upon H→D substitution. This increase is related to the zero point distance between the two pairs of oxygen atoms involved in the two hydrogen bonds, which is different between the O⋯H⋯O and O⋯D⋯O arrangements, within the double minima potential-energy surface associated to the proton tunneling motions.

The observed discrepancies between the experimental and calculated ΔP_{aa} values could be interpreted with the corrections to the C1–C10 distances given in Table 5.

Table 5: r_0 shifts (Δr_0) upon deuteration OD of the distances between the C1 and C10 carbon atoms in AA-DFA.

	$\Delta r_0(\text{C1-C10})$ [mÅ]			
	CT	TT	CG	TG
AA(OD)-DFA	3.5(1) ^[a]	4.7(1)	4.9(1)	3.9(1)
AA-DFA(OD)	7.1(1)	7.1(1)	4.9(1)	6.9(1)
AA(OD)-DFA(OD)	10.0(1)	–	9.3(1)	10.2(1)

[a] Error in parentheses in units of the last digit.

It seems that each OH→OD substitution produces, on the average, a 5 mÅ increase of the distance between the two-component carboxylic acids.

We could estimate the relative populations of the four conformers in the jet from relative intensity measurements of some pairs of nearby μ_a -type lines. We obtained $N_{CT}/N_{CG}/N_{TG}/N_{TT} \approx 12/10/1/1$. As outlined in other papers,^[19] the jet plume is not at the thermodynamic equilibrium, and the relative concentrations of the dimer conformers depend also on the relative concentrations of the conformers of the monomers, such that it is difficult to derive the relative energies. The relative populations are, however, quite far away from what expected from the ab initio relative energies, also taking into account the conformational degeneracy (1 for CT and TT, and 2 for CG and TG). It appears that the T form of the AA monomer is less populated with respect to the relative energy values reported in Ref. [13].

Reasonable values of the dissociation energies of the four forms of the complex can be obtained within a pseudo-diatomic approximation. First the stretching force constant (k_s) is estimated from Equation (4),^[20]

$$k_s = 16\pi^4 (\mu R_{CM})^2 [4B^4 + 4C^4 - (B-C)^2(B+C)^2] / (hD_J) \quad (4)$$

where μ is the pseudo-diatomic reduced mass and R_{CM} ($= 5.005, 5.047, 5.013$, and 5.024 Å for CT, TT, CG, and TG conformers, respectively) is the distance between the centers of mass of the two subunits and D_J is the main centrifugal distortion constant. Then, assuming a Lennard–Jones-type potential to hold for this kind of complex, the dissociation energy is evaluated through Equation (5).^[21]

$$E_D = 1/72 k_s R_{CM}^2 \quad (5)$$

The values $E_D = 48, 50, 61$, and 54 kJ mol^{−1} have been calculated for the CT, TT, CG, and TG species, respectively.

Finally, from the measured tunneling frequencies due to the internal rotation of the -CHF₂ groups in the CG and TG conformers, we could determine the potential-energy surfaces hindering these internal motions. Such a kind of motion should be described with a cyclic function. However, ab initio calculations suggested for both couples of conformers (CG-CT and TG-TT) the shapes given in Figure 3.

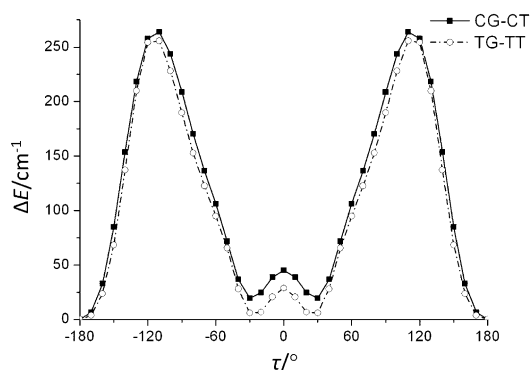


Figure 3. Ab initio potential-energy functions for the internal rotations of the $-\text{CHF}_2$ group in the CG-CT and TG-TT pairs of conformers of AA-DFA.

So we can impute the observed splitting to the low barriers connecting the two equivalent *gauche* forms. In these cases a potential-energy function [Eq. (6)] suitable to include the two equivalent *gauche* minima can be used,

$$V(\tau) = B_2[1 - (\tau/\tau_e)^2]^2 \quad (6)$$

where B_2 and τ are the barrier connecting the two equivalent minima and the H15C14-C10O12 dihedral angle describing the internal rotation of the $-\text{CHF}_2$ group, respectively. Its value is zero at the top of the barrier to the interconversion of the two *gauche* forms, while it is $\pm\tau_e$ at the two minima. We used three pieces of experimental data, the ΔE_{0+0-} tunneling splittings, the values of the P_{cc} planar moments of inertia, defined similarly to P_{aa} , as discussed above, and ΔA_{0+0-} , the changes in the rotational constants A in going from the 0^+ to the 0^- states. The P_{cc} values are mainly useful to estimate the τ_e values, while the ΔE_{0+0-} and ΔA_{0+0-} quantities are mainly related to the barrier heights.

We also allowed for the structural relaxations of several parameters, according to the ab initio indications. These relaxations are expressed by Equation (7).

$$S(\tau) = S_0 + \Delta S(\tau/\tau_e) \quad (7)$$

Details of the specific relaxations are given in the Supporting Information. The obtained results are listed in

Table 6: Flexible model results and potential energy parameters for the internal rotation of $-\text{CHF}_2$ in AA-DFA.

		CG	TG
a) Experimental and calculated data			
P_{cc} [$\text{u}\text{\AA}^2$]	Exp	24.942	23.483
	Cal	24.912	23.450
ΔE_{0+0-} [MHz]	Exp	1.32	3.43
	Cal	1.32	3.52
ΔA_{0+0-} [MHz]	Exp	-0.53	-1.70
	Cal	-0.51	-1.31
b) Determined parameters			
B_2 [cm^{-1}]		102(3)	86(3)
τ_e [$^\circ$]		44.7(3)	47.7(3)

Table 6. One can note that the effects of the *cis* or *trans* arrangement of the allyl group, on the opposite extreme (with respect to the $-\text{CHF}_2$ group) of the dimer, affects considerably the B_2 and τ_e values. Much more significant is the decrease of B_2 with respect to the bare DFA molecule, for which the value $B_2 = 190(10) \text{ cm}^{-1}$ is reported.^[14]

For the calculations we used Meyer's one-dimensional flexible model,^[22] suitable to evaluate vibrational and rotational wavefunctions and eigenvalues. In the flexible model calculations, the range $-\pi/2$ to $\pi/2$ has been resolved into 41 mesh points.

In summary, we investigated the conformational equilibrium in the AA-DFA dimer, obtaining the following results:

- 1) Rotational characterization, for the first time, of four conformers of an adduct of two—considerably heavy—molecules of carboxylic acids.
- 2) Quantitative description of the Ubbelohde effect in dimers of carboxylic acids, which implies, on the average, a 5 mÅ increase of the distance between the two component carboxylic acids for each OH→OD substitution.
- 3) The estimate, from relative intensity measurements, of the relative abundances of the four conformers in the jet.
- 4) An estimate of the dissociation energy for the four dimers, which is in the range of 48–61 kJ mol^{-1} , according to the chemical values well-known for this kind of interaction.
- 5) Tunneling splittings measured for the TG and CG forms allowed the determination of the B_2 barriers to the interconversion of the two *gauche* equivalent minima, which takes place through the internal rotation of the terminal $-\text{CHF}_2$ group.
- 6) Transmission of information through the π system of the eight-atom assembly constituted by the two carboxylic groups: the orientation of the vinyl group in AA influences considerably the B_2 and τ_e values of the $-\text{CHF}_2$ group internal rotation in DFA, miles away from each other. The barrier $B_2 = 102 \text{ cm}^{-1}$ in CG, decreases to 86 cm^{-1} in TG, just because of the *cis* or *trans* orientation of the vinyl group. Such an effect can be observed only with the high-resolution features of pulsed jet FTMW spectroscopy.

Received: September 27, 2013

Revised: October 25, 2013

Published online: November 26, 2013

Keywords: conformation analysis · hydrogen bonds · internal dynamics · rotational spectroscopy · supersonic expansions · Ubbelohde effect

- [1] C. C. Costain, G. P. Srivastava, *J. Chem. Phys.* **1961**, 35, 1903.
- [2] a) L. Martinache, W. Kresa, M. Wegener, U. Vonmont, A. Bauder, *Chem. Phys.* **1990**, 148, 129; b) S. Antolinez, H. Dreizler, V. Storm, D. H. Sutter, J. L. Alonso, *Z. Naturforsch. A* **1997**, 52, 803.
- [3] a) V. V. Matylitsky, C. Riehn, M. F. Gelin, B. Brutschy, *J. Chem. Phys.* **2003**, 119, 10553; b) R. Georges, M. Freytes, D. Hurtmans, I. Kleiner, J. V. Auwera, M. Herman, *Chem. Phys.* **2004**, 305, 187; c) C. Riehn, V. V. Matylitsky, M. F. Gelin, B. Brutschy, *Mol.*

- Phys.* **2005**, *103*, 1615; d) Z. Xue, M. A. Suhm, *J. Chem. Phys.* **2009**, *131*, 054301; e) F. Madeja, M. Havenith, *J. Chem. Phys.* **2002**, *117*, 7162; f) M. Ortlieb, M. Havenith, *J. Phys. Chem. A* **2007**, *111*, 355; g) A. Gutberlet, G. W. Schwaab, M. Havenith, *Chem. Phys.* **2008**, *343*, 158; h) O. Birer, M. Havenith, *Annu. Rev. Phys. Chem.* **2009**, *60*, 263.
- [4] I. Kalkman, C. Vu, M. Schmitt, W. L. Meerts, *ChemPhysChem* **2008**, *9*, 1788.
- [5] A. M. Daly, K. O. Douglass, L. C. Sarkozy, J. L. Neill, M. T. Muckle, D. P. Zaleski, B. H. Pate, S. G. Kukolich, *J. Chem. Phys.* **2011**, *135*, 154304.
- [6] M. C. D. Tayler, B. Ouyang, B. J. Howard, *J. Chem. Phys.* **2011**, *134*, 054316.
- [7] G. Feng, L. B. Favero, A. Maris, A. Vigorito, W. Caminati, R. Meyer, *J. Am. Chem. Soc.* **2012**, *134*, 19281.
- [8] L. Evangelisti, P. Eciija, E. J. Cocinero, F. Castaño, A. Lesarri, W. Caminati, R. Meyer, *J. Phys. Chem. Lett.* **2012**, *3*, 3770.
- [9] G. Feng, Q. Gou, L. Evangelisti, Z. Xia, W. Caminati, *Phys. Chem. Chem. Phys.* **2013**, *15*, 2917.
- [10] Q. Gou, G. Feng, L. Evangelisti, W. Caminati, *J. Phys. Chem. A* **2013**, DOI: 10.1021/jp407175r.
- [11] Q. Gou, G. Feng, L. Evangelisti, W. Caminati, *J. Phys. Chem. Lett.* **2013**, *4*, 2838.
- [12] A. R. Ubbelohde, K. J. Gallagher, *Acta Crystallogr.* **1955**, *8*, 71.
- [13] K. Bolton, D. G. Lister, J. Sheridan, *J. Chem. Soc. Faraday Trans. 2* **1974**, *70*, 113.
- [14] B. P. van Eijck, A. A. J. Maagdenberg, G. Janssen, T. J. van Goe-them-Wiersma, *J. Mol. Spectrosc.* **1983**, *98*, 282.
- [15] Gaussian03 Revision B.01, M. J. Frisch et al., Gaussian Inc. Pittsburgh, PA, **2003**.
- [16] S. F. Boys, F. Bernardi, *Mol. Phys.* **1970**, *19*, 553.
- [17] H. M. Pickett, *J. Mol. Spectrosc.* **1991**, *148*, 371.
- [18] J. K. G. Watson in *Vibrational Spectra and Structure*, Vol. 6 (Ed.: J. R. Durig), Elsevier, New York, **1977**, pp. 1–89.
- [19] See, for example, W. Caminati, J. C. López, S. Blanco, S. Mata, J. L. Alonso, *Phys. Chem. Chem. Phys.* **2010**, *12*, 10230.
- [20] D. Millen, *Can. J. Chem.* **1985**, *63*, 1477.
- [21] S. E. Novick, S. J. Harris, K. C. Janda, W. Klemperer, *Can. J. Phys.* **1975**, *53*, 2007.
- [22] a) R. Meyer, *J. Mol. Spectrosc.* **1979**, *76*, 266; b) R. Meyer, W. Caminati, *J. Mol. Spectrosc.* **1991**, *150*, 229.